Single Photon Interference

Kyungmin Yu*
Department of Materials Science and Engineering,
Seoul National University
1, Gwanak-ro, Gwanak-gu, Seoul, Republic of Korea
E-mail: yukm0227@snu.ac.kr
(Dated: May 2, 2024)

A double-slit experiment for multiple and single photon cases confirmed the wave-particle duality of light. For the multiple photon case, light scattered through the double slit and showed the interference pattern enveloped by the scattering pattern, which is analogous to the theory of wave optics. Also, light showed the scattering pattern when it passed through the single slit as predicted in the theory of wave optics. These patterns appeared identically in the single photon case, which proved that the wave-like property is an intrinsic property of the photon. To improve the accuracy of the fitting, some corrections such as bandwidth or Fresnel diffraction were conducted.

I. INTRODUCTION

The Wave-particle duality of light is an important topic in modern physics. Without understanding the properties of light, it is impossible to analyze many physical phenomena properly. [1] There have been a lot of trials and errors to investigate the wave or particle properties of light. One of the most well-known experiments is the double-slit experiment, which was initially conducted by British physicist, Thomas Young. Based on this experiment, the wave-like properties of light were proved. After Young's generation, the same result was obtained even for the single photon interference. Due to the result, it was believed that the wave-particle duality of light is a unique, intrinsic property of light. In this experiment, the main goal is to reproduce the double-slit experiment for an ordinary case and a single photon case. The double slit experiment is conducted with LASER and PMT (Photomultiplier Tube), which enables the single photon case experiment.

A. Background: Interference Theory

There are two regimes for the diffraction through obstacles. The first case is the limit that the dimension of the obstacles is much smaller than the distance to the screen. This regime is called Fraunhofer diffraction, and the incident light can be approximated to the plane wave since the obstacle is small enough to neglect its detailed structure. On the contrary, Fresnel diffraction accounts for the case that the obstacle is large enough to affect the plane wave approximation. In this case, the incident light cannot be approximated to the plane wave, and a more complicated theory must be introduced. Given that the usual double-slit experiment uses an apparatus whose slit size is small enough to apply the Fraunhofer diffraction theory, the latter regime will not be considered in this experiment. Applying the classical optics theory, the amplitude $A(x', y')$ of the electromagnetic wave at a certain point on the screen (x', y') is the form of Fourier transform like (1), where $f(x, y)$ is an amplitude function of the obstacles. [2]

$$A(x', y') \propto e^{ikr} \iint f(x, y) e^{-ik(xx'+yy')/r} dxdy \tag{1}$$

Based on the theory of wave optics [2], the intensity profile can be simplified. Assume that the monochromatic light interferes through the double slit with distance d and slit width a. If the slit width is negligible compared to the slit distance, the intensity profile on the screen is like (2), where I_0 is the intensity at the center point. Note that there is an approximation of the distance to the screen is much larger than d.

$$I(\theta) = I_0 \cos^2 \gamma, \gamma = \frac{\pi d \sin\theta}{\lambda} \tag{2}$$

To account the finite slit width, the effect of diffraction by the finite-width slit must be included. Based on the phasor method, the intensity profile can be obtained as (3), where I_0 is the intensity at the center point.

$$I(\theta) = I_0 \frac{\sin^2 \beta}{\beta^2}, \beta = \frac{\pi a \sin\theta}{\lambda} \tag{3}$$

For the finite-width double slit, the intensity profile is the product of two terms in (2) and (3). Namely, the intensity profile is in form of (4), where γ and β are defined in (2) and (3).

$$I(\theta) = I_0 \frac{\sin^2 \beta}{\beta^2} \cos^2 \gamma \tag{4}$$

The ideal monochromatic light was considered above, however, obtaining the perfect monochromatic light is impossible. Therefore, the line width of light must be considered to improve the accuracy of the experiment. For the non-monochromatic light, the distribution of wave number, $g(k)$ is given, where the normalization

* Also at Department of Physics and Astronomy, Seoul National University. (Double major)

condition (5) holds. This distribution is called spectral strength. [2]

$$\int_0^\infty g(k)dk = 1 \tag{5}$$

If the bandwidth is known to be small enough, the intensity function $g(k)$ can be approximated as a Lorentzian function with respect to wavelength, like (6).

$$g(k) = \frac{\gamma}{\pi((\lambda-\lambda_0)^2+\gamma^2)}, \lambda = \frac{2\pi}{k} \tag{6}$$

Accounting for the spectral strength, the intensity profile changes like (7), where the definition of γ and β is identical to (2) and (3). Note that γ and β is function of wave number k.

$$I(\theta) = \int_0^\infty I_0 \frac{\sin^2\beta}{\beta^2}\cos^2\gamma g(k)dk \tag{7}$$

B. Background: Photomultiplier tube

Photomultiplier tube, shortly PMT amplifies very weak light signals into measurable voltage signals. Even PMT can detect a single photon. In PMT, the incident photon makes the cathode emit an electron due to the photoelectric effect. The emitted electron is accelerated through dynode and collides with another electrode to make the electrode emit more electrons. This process is repeated several times, then the measurable magnitude of the current is generated in the anode. To control the PMT well, the acceleration voltage must be controlled carefully. The single-photon signal will be lost before amplification if the acceleration voltage is too low. On the contrary, noises will be too high with too high acceleration voltage. Note that PMT is very vulnerable to light since it is designed to detect extremely weak light signals. [3]

II. MATERIALS AND METHODS

A. Overview of the Apparatus

'Two-Slit Interference, One Photon at a Time' apparatus (TeachSpin, Inc.) was prepared for this experiment. It is composed of mainly three parts: light sources (a LASER and a bulb), U-channel, and detectors (a photodiode and PMT). The LASER and the photodiode are used for the ordinary interference experiment, while the bulb and the PMT are used for the single photon case. Detectors can be connected to a multimeter, a Pulse Counter and Interval Timer (PCIT), or an oscilloscope to measure physical quantities. Two single slits, one blocker slit, and three types of double slits (No. 14, No. 15, No. 16) were prepared, and they can be attached inside the U-channel with a magnet. The position of the blocker slit and the detector slit can be adjusted by screws. According to the handbook, the dimension of the three slits are as follows.

TABLE I. The dimension of the three slits.

	Slit Spacing (d) [μm]	Slit Width (a) [μm]
Slit No. 14	356	85
Slit No. 15	406	85
Slit No. 16	457	85

B. Alignment

To proceed with the experiment properly, each part of the apparatus must be aligned well. The first step was aligning the LASER to reach the screen. After the LASER was fixed well, an adjusting screw was used to control the direction of the LASER. Then, the source slit was located in front of the LASER, which must not be tilted or block the light. The detector slot was located in front of the detector in the same way. After that, the double slit No. 14 was located in the middle of two single slits. The intensity profile was skimmed whether it matches up with the theoretical double slit profile.

Finally, the blocker slit was inserted and its angle was aligned carefully. When the blocker slit is moved, each slit in the double slit must be closed parallel to the direction of the slit. After inserting the blocker slit, the measured voltage according to its position was plotted to check good alignment. For the three slits, the plot is shown in FIG. 1. The lowest voltage is the state that two slits are all closed by the blocker slit. The jumps of the voltage show the opening of each slit by position change of the blocker slit. The steep change of the voltage at jumping points implies that the blocker slit shields each slit in parallel to the direction of the slit. Two flat levels appear between each jump, which are the states where one or two slits are open. Especially, the length of the lower level can be applied to estimate the spacing of the double slit. Referring to TABLE I, the spacing of two slits increases as the serial number increases. In FIG. 1, this tendency can be checked by comparing the length of the lower level. The voltage ratio of the two levels is theoretically $4:1$ according to the equation (2) and (3), assuming the central maxima. However, in reality, the position of the detector is not exactly the central maxima for single slit. Therefore, the actual ratio is smaller than $4:1$.

During the overall process, the alignment was checked by a paper card showing the center line of the U-channel. The LASER image formed on the center line implies good alignment. This alignment process was performed after changing the double slit or the light source. Describing the process in the following section, the alignment procedure is assumed to be finished.

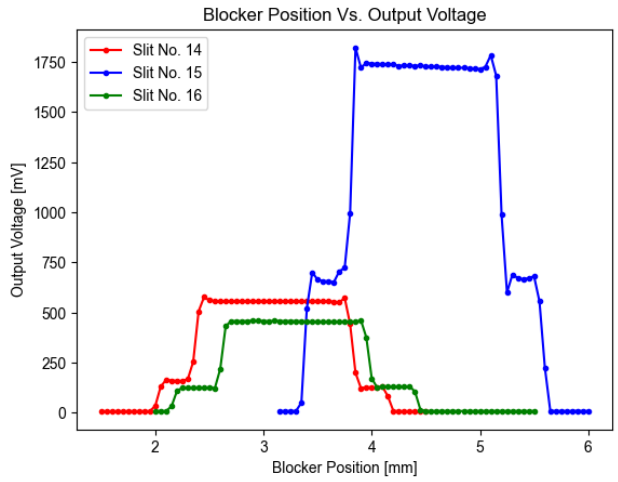

FIG. 1. Measured voltage according to the blocker position.

C. Multiple Photon Interference

To measure the signal from the photodiode, its output terminal was connected to the multimeter to show the voltage value. Before the double slit interference experiment, the alignment of the blocker slit was verified by plotting the voltage to the position of the blocker slit. Then, the blocker slit was moved to expose the whole double slit. The detector slit was located at 1.000 mm, then moved to the right with an interval of 0.050 mm until 9.000 mm. The voltage was read at every interval, and then the voltage to the position was plotted. The double-slit experiment was conducted for three double slits. Moving the blocking slit, it is possible to block only one side of the double slit to make the single slit or block one side partially to make the asymmetric slit. The same data was obtained for the single slit and the asymmetric slit. Based on the obtained data, the line width of the LASER can be estimated by regression technique.

D. Single Photon Interference

To measure the number of photons, the output terminal of PMT was connected to the PCIT. Also, the light source was changed to a bulb. First, the drive voltage of the PMT was estimated by comparing the dark rate and the bright rate. Within the voltage range, PMT can function properly with a low magnitude of noise. Then, the output terminal of PMT was divided and connected to the PCIT and the oscilloscope. Comparing two outputs, the threshold voltage of PMT (the minimum voltage that PMT counts as a pulse) could be set properly. After setting these parameters, double and single-slit interference were measured in the same sequence as the multiple photon case. The asymmetric slit experiment was omitted.

III. RESULT

A. Multiple Photon Interference

1. *Double-Slit Experiment*

The Double-slit experiment was conducted for slits No. 14, No. 15, and No. 16. The fitting function and parameters are as follows. Note that the fitting parameters are distinguished with a subscript 0.

$$\begin{aligned} &f(x; I_0, a_0, b_0, c_0, C_0) \\ &\quad = I_0 \frac{\sin^2(a_0(x-b_0))}{(a_0(x-b_0))^2} \cos^2(c_0(x-b_0)) + C_0 \end{aligned} \tag{8}$$

Comparing (8) with (2), a_0 and b_0 have a relationship like (9) with the approximation of $L \gg x$. Also, c_0 and b_0 have a relationship like (10).

$$a_0(x-b_0) = \frac{\pi a \sin\theta}{\lambda} \simeq \frac{\pi a(x-x_0)}{L\lambda} \tag{9}$$

$$c_0(x-b_0) = \frac{\pi d \sin\theta}{\lambda} \simeq \frac{\pi a(x-x_0)}{L\lambda} \tag{10}$$

Therefore, the fitting parameters a_0, b_0 and c_0 are expressed as (11). Note that the distance between the slit and the detector is $L = 500$ mm and the wavelength of the LASER is λ =670 nm according to the handbook of the apparatus.

$$a_0 = \frac{\pi a}{L\lambda}, b_0 = x_0, c_0 = \frac{\pi d}{L\lambda} \tag{11}$$

The fitting was conducted with MATLAB Curve Fitting Toolbox (Mathworks, Inc.). After loading the raw data, the naive form of the raw data was checked. Due to the finite dimension of the detector slit, the anomalies occur far from the central maxima. The detector slit does not cover the detector perfectly when the slit is located too far from the center. Therefore, the raw data was trimmed appropriately to exclude the anomalies. After the preprocessing, the initial values and the range of the parameters were tuned to find the global minima. Note that MATLAB Curve Fitting Toolbox automatically calculates not only the value of optimized parameters but also the 95 % confidence intervals for each parameter.

For slits No. 14, No. 15, and No. 16, the fitting result is shown in Fig. 2a to Fib. 2c. The R^2 values, fitting parameters, and their 95 % confidence intervals are enumerated in TABLE II. Since the R^2 values are higher than 0.994 for all the three slits, the fitting seems to be reasonable. Applying (11), it is possible to estimate the spacing and the width of the double slit. The estimated dimensions of the slits are shown in TABLE II, where d and a are the spacing and the gap of the slit, respectively. It can be checked that the estimated values of spacing and width are comparable to the known dimension of slits in TABLE I.

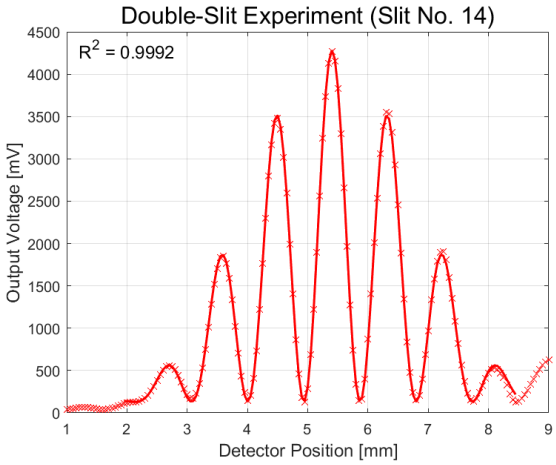

FIG. 2a. The result of the double-slit experiment for the slit No. 14 in the multiple photon case.

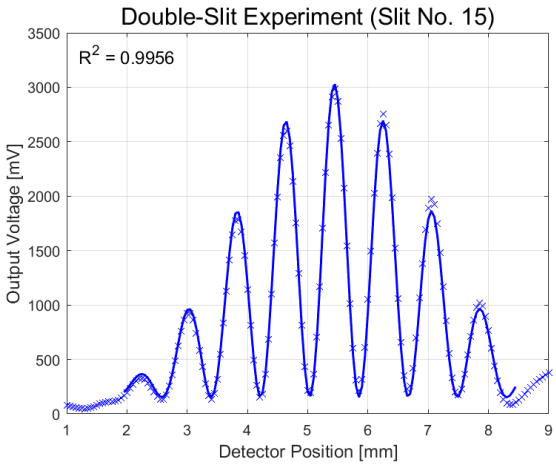

FIG. 2b. The result of the double-slit experiment for the slit No. 15 in the multiple photon case.

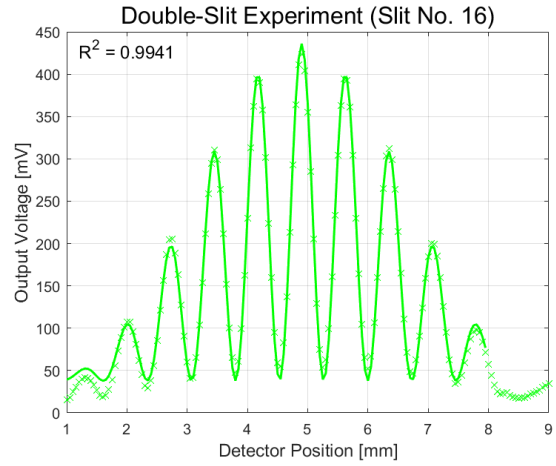

FIG. 2c. The result of the double-slit experiment for the slit No. 16 in the multiple photon case.

TABLE II. The values of R^2, fitting parameters and 95 % confidence intervals for the double-slit experiment in the multiple photon case.

	Slit No. 14	Slit No. 15	Slit No. 16
R^2	0.9992	0.9956	0.9941
I_0 [mV]	4153 ± 21	2879 ± 34	398.1 ± 5.2
a_0 [mm^{-1}]	0.8381 ± 0.0048	0.7492 ± 0.0100	0.7237 ± 0.0137
b_0 [mm]	5.403 ± 0.001	5.442 ± 0.002	4.899 ± 0.002
c_0 [mm^{-1}]	3.370 ± 0.003	3.843 ± 0.006	4.295 ± 0.007
C_0 [mV]	130.4 ± 9.6	152.5 ± 16.0	37.89 ± 2.46
d [µm]	359.4 ± 0.4	409.8 ± 0.7	458.0 ± 0.7
a [µm]	89.37 ± 0.51	79.89 ± 1.07	77.17 ± 1.14

2. *Single-Slit Experiment*

The single-slit experiment was conducted for both sides of slit No. 14. The fitting function and parameters are as follows. Note that the fitting parameters are distinguished with a subscript 0.

$$f(x; I_0, a_0, b_0, C_0) = I_0 \frac{\sin^2(a_0(x - b_0))}{(a_0(x - b_0))^2} + C_0 \qquad (12)$$

The relation in (11) still holds. The fitting was conducted with MATLAB Curve Fitting Toolbox (Mathworks, Inc.) similar to the double-slit fitting.

For the left and right slit of slit No. 14, the fitting result is shown in Fig. 3. As shown in Fig. 3, the anomalies occur when the detector is far from the central maxima, as in the double-slit experiment. Therefore, the fitting was conducted for the region near the central maxima. The bold line shows the fitting function and the region of the fitting. The fitting parameters and the coefficient of determination are shown in TABLE III. The 95 % confidence intervals of fitting parameters are calculated. Applying (11), the width of the left slit is 95.00(248) µm, and the width of the right slit is 92.50(77) µm. The 95

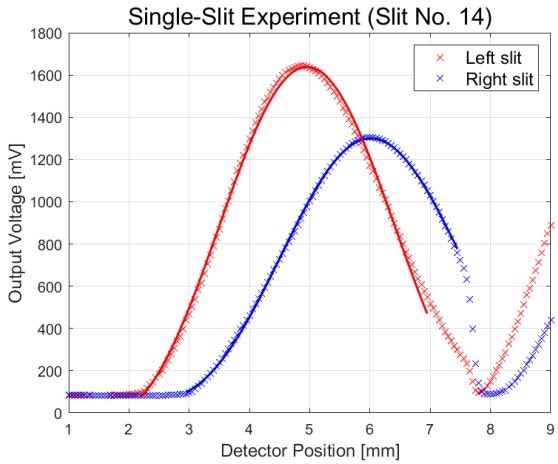

FIG. 3. The result of two single-slit experiments for the slit No. 14 in the multiple photon case.

TABLE III. The values of R^2, fitting parameters and 95 % confidence intervals for the single-slit experiment in the multiple photon case.

	Left Slit	Right Slit
R^2	0.9965	0.9996
I_0 [mV]	1678 ± 45	1240 ± 9
a_0 [mm^{-1}]	0.8907 ± 0.0233	0.8675 ± 0.0072
b_0 [mm]	4.955 ± 0.010	6.014 ± 0.005
C_0 [mV]	-39.24 ± 48.40	60.02 ± 9.47
a [µm]	95.00 ± 2.48	92.50 ± 0.77

% confidence interval of the left slit contains the right slit, while the 95 % confidence interval of the right slit does not. Therefore, it can be claimed that two slits have slightly different widths. This testing method will be conducted once again for the single photon case in the following section.

3. *Asymmetric Slit Experiment*

The blocker slit was located to partially shield the right slit of the slit No. 14. Based on FIG. 1, the blocker position was set to be 2.33 mm and 2.38 mm. The detector was moved and the position-wise voltage was obtained like FIG. 4. A suitable fitting for the asymmetric slit experiment will be discussed in the following section.

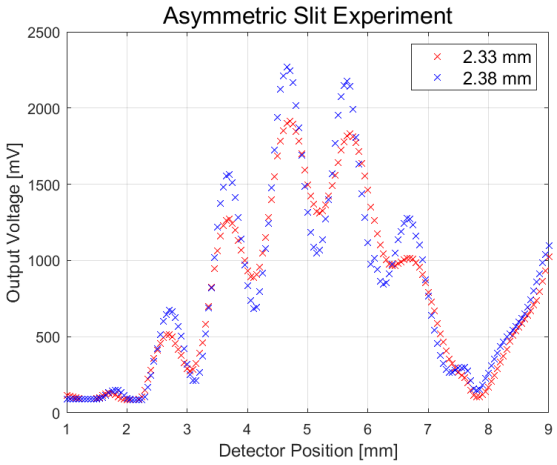

FIG. 4. The result of the asymmetric slit experiment.

B. Single Photon Interference

1. *PMT Calibration*

If the drive voltage is too low, the incident photon can't be amplified by the drive voltage. On the contrary, the noise becomes significant if the drive voltage is too high. Therefore, the drive voltage must be tuned well to progress the experiment properly. The upper boundary of the drive voltage was estimated by measuring the photon count without any light source increasing the drive voltage. If the photon count exceeds a certain value, it implies that the drive voltage is excessive. Similarly, The lower boundary of the drive voltage was estimated by measuring the photon count with a weak light source. The drive voltage does not amplify the incident photon well if the photon count is lower than a certain value. Note that the certain value was set to be 15 photons. This value was set as an adequate number to avoid a large error due to too low photon counts.

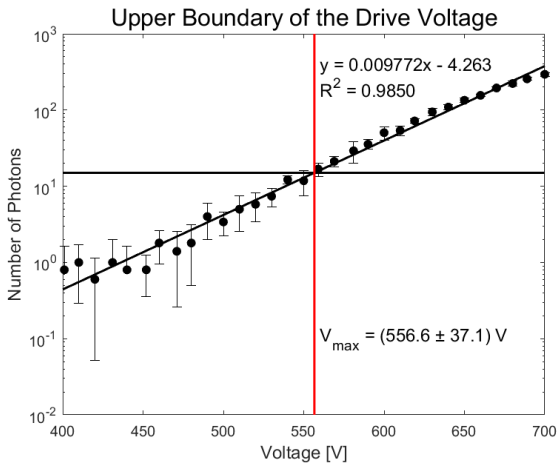

FIG. 5a. The upper boundary of the drive voltage estimated from the linear trend line.

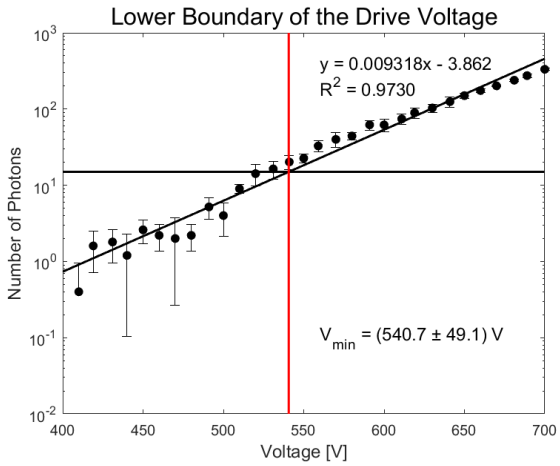

FIG. 5b. The lower boundary of the drive voltage estimated from the linear trend line.

The number of photons increases exponentially as the drive voltage increases. Therefore, the number of photons was plotted with respect to the drive voltage in the log scale. A linear trend line was shown and the drive voltage when the number of photons is 15 was interpolated. With this method, the upper and lower boundary of the drive voltage was obtained as shown in FIG. 5a and FIG. 5b,

respectively. The linear trend line (thick black line), as well as the 1σ error bar (thin black line), were shown. The boundary of the drive voltage is indicated by a red line.

Since the upper boundary of the drive voltage is 556.6(371) V and the lower boundary of the drive voltage is 540.7(491) V, the drive voltage was set to be 550 V for the following experiments.

The threshold voltage of the PCIT was tuned based on the comparison between the output of an oscilloscope and the PCIT. The number of photons and the number of signals detected in the oscilloscope were set to be as similar as possible. The threshold voltage of the PCIT was set as 0.01 V.

2. *Bulb - Detector Calibration*

After removing the blocker and the double slit, the number of photons was measured moving the position of the detector slit. Since the source slit is a single slit, the fitting with the fitting function (12) was conducted. The result is shown in FIG. 7 with the 1σ error bar. Based on the fitting function and (11), the central maximum point was found to be 5.365(7) mm. (Note that the error range is the 95 % confidence interval.) Due to the dimension of the detector slit, the anomaly occurred over 8.0 mm. Therefore, the anomaly was trimmed and the fitting was conducted. Also, the width of the source slit was calculated to be 106.9(7) µm based on (11), with $L = 827$ mm and $\lambda = 546$ nm. The calculated width is comparable to that of TABLE III.

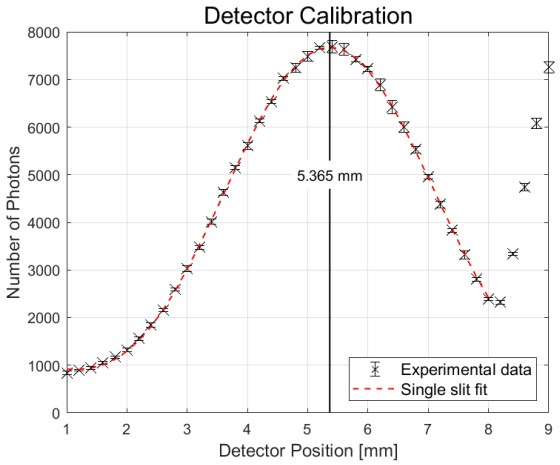

FIG. 6. The number of photons with respect to the position of the detector slit.

Subsequently, at the central maximum point obtained in FIG. 7, the number of photons was measured with different bulb intensities. Then, the exponential fitting was conducted to obtain the parameters. The 1σ error bar and the 95 % confidence interval of each parameter were shown.

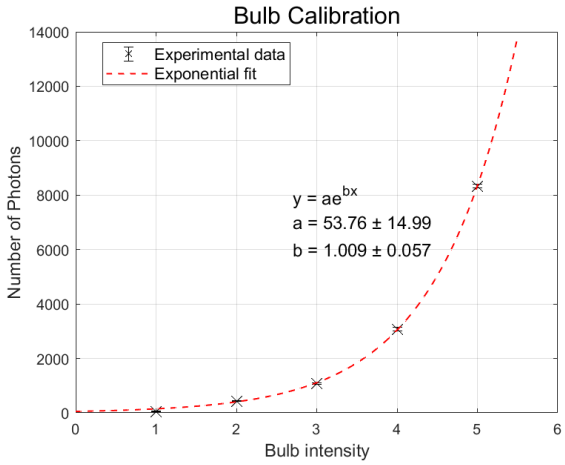

FIG. 7. The number of photons with respect to the intensity of the bulb.

3. *Double-Slit Experiment*

The double-slit experiment for the single photon case was analyzed in the same method as the multiple photon case. The slit No. 14 was only used while the intensity of the bulb was changed. The experimental data with 1σ error bar and the fitting function are shown in FIG. 8a and FIG. 8b. The fitting function is given in (11), and the optimized parameters are enumerated in TABLE IV.

4. *Single-Slit Experiment*

The single-slit experiment for the single photon case was analyzed in the same method as the multiple photon case. Two sides of the slit No. 14 were investigated with a bulb intensity of 5. The experimental data with 1σ error bar and the fitting function are shown in FIG. 9. The fitting function is given in (11), and the optimized parameters are enumerated in TABLE V. The error bar indicating 1σ error range was shown as black, bold lines.

It can be checked that the 95 % confidence intervals of the left and the right slit contain each other. Therefore, it can be concluded that the two slits have identical widths at 95 % significance level. This result is not the same as that of the multiple photon case. For the single photon case, 95 % confidence intervals of fitting parameters are quite wide due to a big fluctuation. Wide confidence intervals imply that the statistical significance of the testing is much lower than that of the multiple photon case. Based on two statistical tests for the multiple and single photon cases, the two slits in the slit No. 14 have slightly different widths.

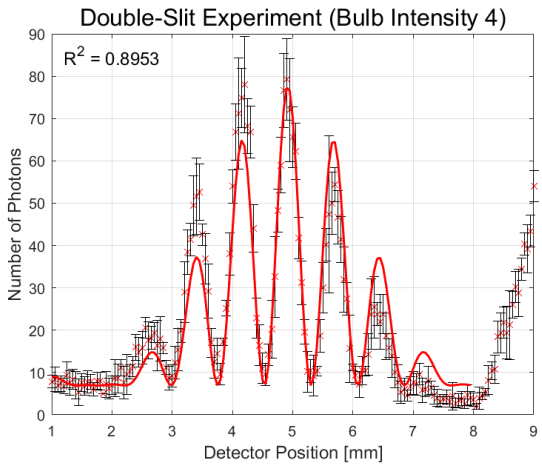

FIG. 8a. The result of the double-slit experiment for the slit No. 14 and the bulb intensity 4 in the single photon case.

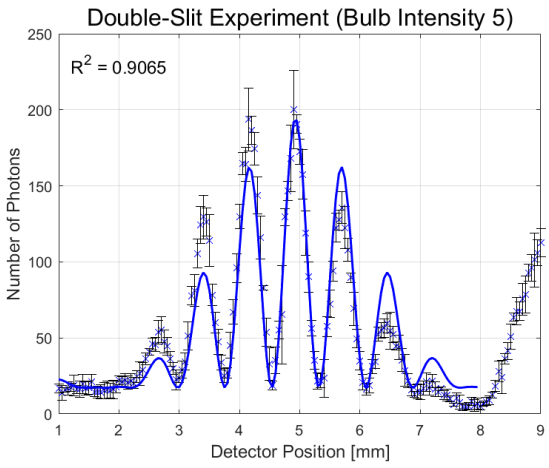

FIG. 8b. The result of the double-slit experiment for the slit No. 14 and the bulb intensity 5 in the single photon case.

TABLE IV. The values of R^2, fitting parameters, and 95 % confidence intervals for the double-slit experiment in the single photon case.

	Intensity 4	Intensity 5
R^2	0.8953	0.9065
I_0	70.74 ± 4.26	177.2 ± 10.0
a_0 [mm^{-1}]	0.9968 ± 0.0648	0.9914 ± 0.0606
b_0 [mm]	4.919 ± 0.010	4.929 ± 0.009
c_0 [mm^{-1}]	4.061 ± 0.050	4.027 ± 0.047
C_0	6.933 ± 1.532	17.26 ± 3.62
d [μm]	352.9 ± 4.3	349.9 ± 4.1
a [μm]	86.62 ± 5.67	86.15 ± 5.27

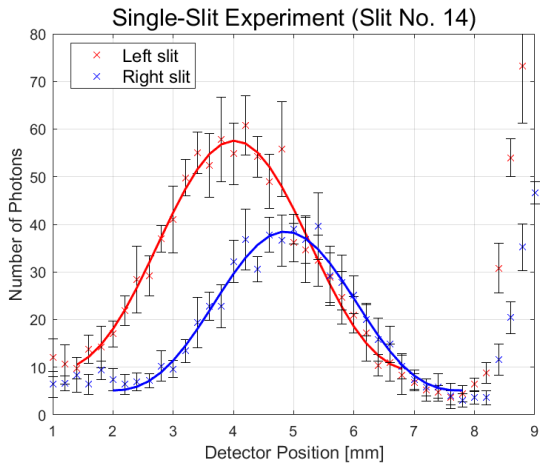

FIG. 9. The result of two single-slit experiments for the slit No. 14 in the single photon case.

TABLE V. The values of R^2, fitting parameters and 95 % confidence intervals for the single-slit experiment in the single photon case.

	Left Slit	Right Slit
R^2	0.9731	0.9996
I_0 [mV]	48.43 ± 4.25	33.38 ± 2.28
a_0 [mm^{-1}]	1.024 ± 0.112	1.098 ± 0.092
b_0 [mm]	4.013 ± 0.062	4.864 ± 0.061
C_0 [mV]	9.139 ± 4.371	5.110 ± 1.892
a [μm]	88.98 ± 9.73	95.41 ± 7.91

IV. DISCUSSION

A. Consideration of the Bandwidth

The LASER in the experiment has a slight bandwidth, and the fitting accuracy can be improved when the bandwidth is considered. Since the LASER emits almost monochromatic light, the spectral strength was approximated as a Lorentzian function like the equation (6). By a numerical integration technique, the bandwidth of the LASER was obtained by a regression model. The result is shown in FIG. 10. The calculated maximum wavelength and FWHM (Full-Width at Half Maximum) is 650.0(108) nm. According to the handbook of the apparatus, the wavelength of LASER is 670(20) nm. It can be checked that the regressed value and the value in the handbook matches well within a small error.

Including the bandwidth, the double-slit experiment in the multiple photon case was analyzed. The result is shown in FIG. 11a. Compared to the fitting that does not consider the bandwidth in FIG. 2a, the value of determination coefficient decreased slightly. However, it must be highlighted that the fitting equation in FIG. 11a does not include the constant term C_0. In the fitting equation (8), the constant term C_0 is included to account for possible noise detected in the photodiode. However, the

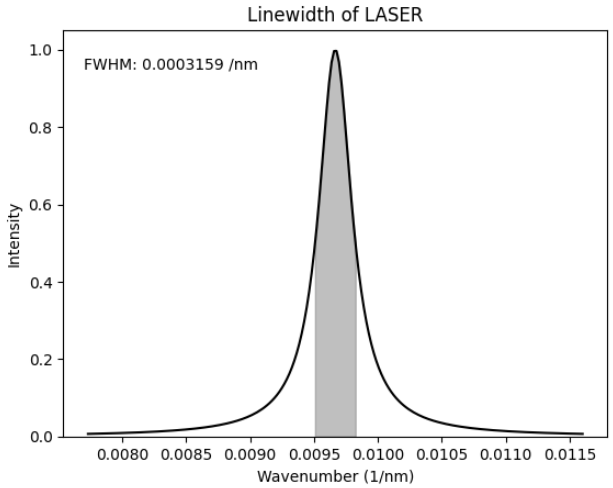

FIG. 10. The bandwidth of the LASER light.

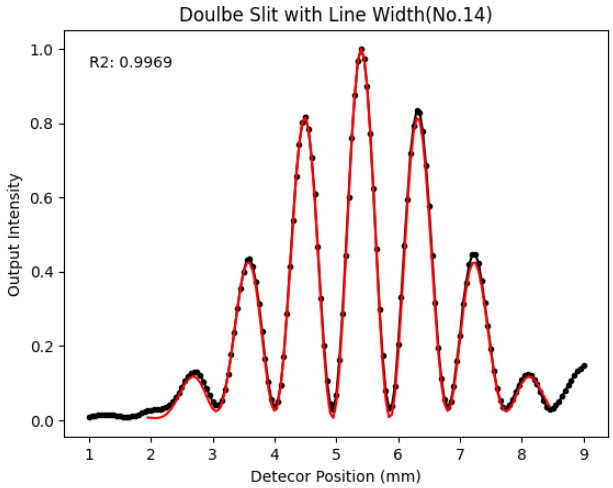

FIG. 11a. Bandwidth correction for the slit No. 14.

constant term may cause an overfitting when the constant term has a value which is too large to account for the noise. Therefore, to fit the experimental data without the constant term is an important issue. The consideration of the bandwidth can be a breakthrough. In the raw data, the observed intensity does not be zero at the minima. This phenomenon occurs because the LASER does not emit perfect monochromatic light. If the bandwidth is considered, the intensity at the minima can be corrected. In FIG. 11a, the minima of fitting function is not perfectly zero due to the bandwidth effect, and it matches well with the experimental points. Therefore, it can be concluded that the fitting accuracy was improved by consideration of the bandwidth, although the determination coefficient decreased. The fitting result including the bandwidth effect for the slits No. 15 and No. 16 are also shown in FIG. 11b and 11c. In this case, the minima deviate from zero much more than the slit No. 14. Nevertheless, the determination coefficient is higher than 0.96 without the constant term. However, the bandwidth correction does not fully account for the intensity of minima, which is clearly shown in FIG. 11c, nearby the central maximum. This mismatch seems to be occurred by noise, which makes the intensity of minima nonzero. However, adding the constant term without any constraint may cause an overfitting as explained above. For the more accurate analysis, the scale of noise must be estimated first, and the range of constant term must be constrained based on this scale.

In the same way, the bandwidth correction was conducted for the single photon case. The wavelength in the handbook is 546(10) nm, and the regressed wavelength is 513.2(59) nm. The result of the bandwidth correction was shown in FIG. 12.

For the double-slit experiment with the bulb intensity 5 and the slit No. 14, the fitting including the bandwidth correction was conducted. The result is shown in FIG. 13. Since the noise is very significant in the single pho-

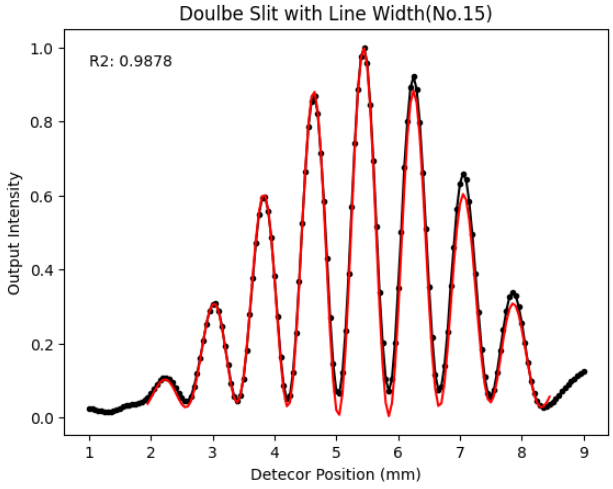

FIG. 11b. Bandwidth correction for the slit No. 15.

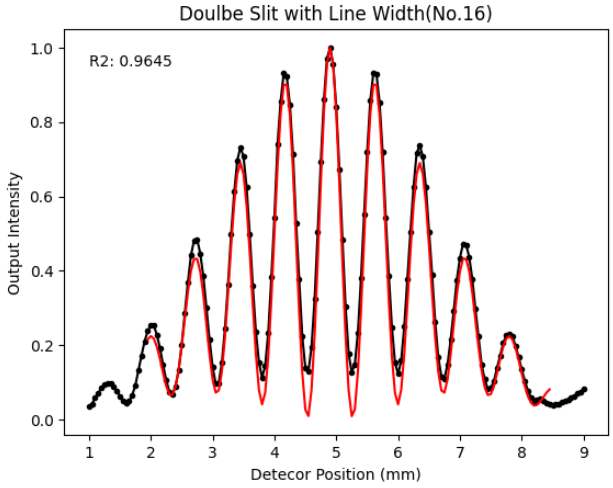

FIG. 11c. Bandwidth correction for the slit No. 16.

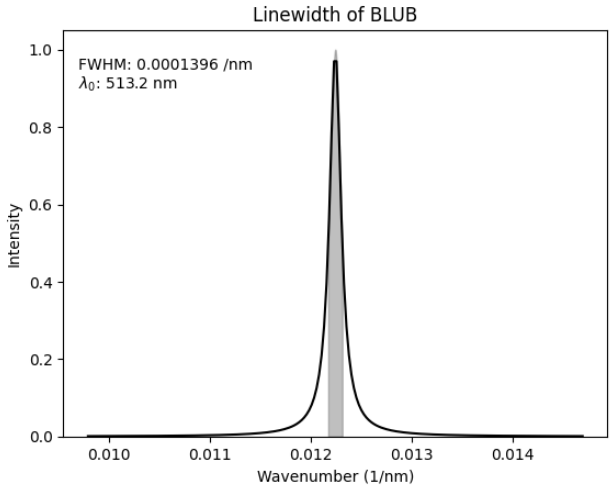

FIG. 12. The bandwidth of the bulb light.

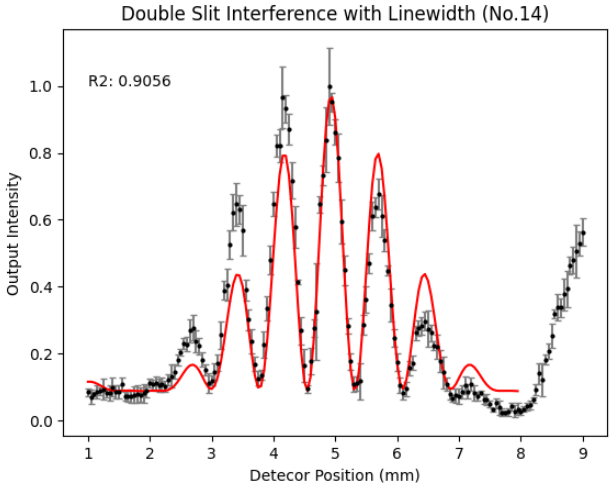

FIG. 13. Bandwidth correction for the slit No. 14 and bulb intensity 5.

ton case, the constant term was included in the fitting function.

Comparing FIG. 8b and FIG. 13, the determination coefficient is not significantly improved. The regressed bandwidth of the bulb was much smaller than that of the LASER, and the effect of correction was small. Nevertheless, the intensity at the minima is still non-zero for the single photon case. The first reason of this fluctuation is the inevitable noise. Since the PMT is very sensitive and this experiment deals with the single photon case, the inevitable noise may be generated by a certain source. The other reason is a decoherence of the light source. Unlike the LASER, the light emitted by the bulb is not coherent. The minima points are determined by the relationship that a path difference to a certain point is an integer multiple of a wavelength. However, if the light source is not coherent or the bandwidth effect is significant, this relationship does not hold anymore. Therefore, decoherence of the light source and the bandwidth effect both make the minima nonzero. However, considering the decoherence effect quantitatively is very challenging since the explicit relationship of the decoherence is unknown.

To sum up, it is essential to consider the bandwidth effect to improve the fitting accuracy. The constant term can be included simultaneously with the bandwidth effect, however, its range must be tuned carefully to avoid the overfitting. Also, for the bulb, the decoherence effect is much larger than the bandwidth effect. The suitable model that contains the decoherence effect need to be developed further.

B. Fresnel diffraction

Fraunhofer interference theory was applied in the fitting equation. However, in reality, the approximation in Fraunhofer theory does not match well. Therefore, the more general theory must be introduced to describe this experiment accurately. Fresnel diffraction theory does not approximate the wave as a plane wave, and gives more accurate result. To construct the model based on Fresnel theory, the dimension of the apparatus was parametrized like FIG. 14.

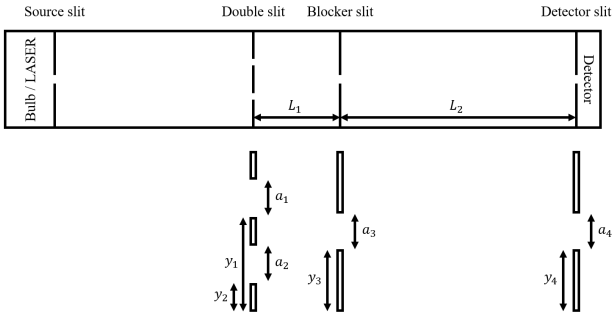

FIG. 14. The parameters that express the dimension of the apparatus.

In FIG. 14, The perfect alignment in the source slit was assumed. Also, since the distance between the light sourse and the double slit is much larger than the slit size, the electric field was approximated to be uniform at the double slit. Then, by Fresnel theory, the electric field at the blocker slit is like (13). y_b denotes the position at the blocker slit, which is measured from the lower side of the apparatus.

$$E_b(y_b) = E_0 \int_{y_1}^{y_1+a_1} \frac{\exp(ik\sqrt{L_1^2+(y_b-y)^2})}{\sqrt{L_1^2+(y_b-y)^2}}dy + E_0 \int_{y_2}^{y_2+a_2} \frac{\exp(ik\sqrt{L_1^2+(y_b-y)^2})}{\sqrt{L_1^2+(y_b-y)^2}}dy \tag{13}$$

In the same way, the electric field at the detector slit can be calculated like (14). y_d denotes the position at the blocker slit, which is measured from the lower side of the apparatus.

$$E_d(y_d) = \int_{y_3}^{y_3+a_3} E_b(y) \frac{\exp(ik\sqrt{L_2^2 + (y_d - y)^2})}{\sqrt{L_2^2 + (y_d - y)^2}} dy \tag{14}$$

Then, the intensity profile can be obtained by squaring the electric field at the detector slit. To apply the final equation, some computational methods such as numerical integration technique and optimization technique is required. The intensity profile of the asymmetric double slit in FIG. 4 was fitted. The fitting was conducted for the data of which blocker position is 2.38 mm, and the fitting result is shown in FIG. 15.

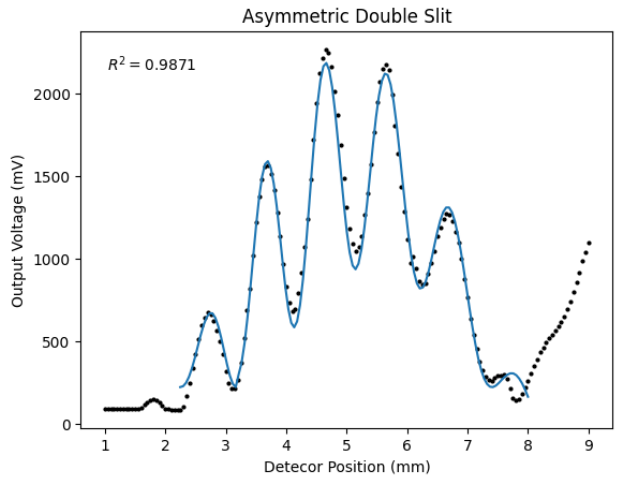

FIG. 15. The fitting for the asymmetric double slit based on Fresnel diffraction model.

A high R^2 value of the fitting shows that Fresnel diffraction model predicts the experimental result very well. It is very challenging to describe the intensity profile of the asymmetric double slit solely using a basic theory. Fresnel diffraction model can make a breakthrough for predicting the intensity profile of the asymmetric double slit. Fresnel diffraction model is very meaningful since every double slit intrinsically has an asymmetry. For instance, the widths of two slits in the slit No. 14 were found to be statistically different, as described in the previous section. In other words, Fresnel diffraction model is required to predict the intensity profile including the intrinsic asymmetry of the double slit. However, Fresnel diffraction model requires much computational costs and time, since it includes some numerical integrations and many parameters. Also, finding the global minimum point is very challenging. Actually, to find the optimized parameters, brute-force method need to be applied. The initial values and hyperparameters of the gradient descent need to be tuned manually to make the fitting converge. Therefore, the trade-off relationship between computational costs and fitting accuracy must be considered, then the appropriate method for the fitting need to be selected.

V. CONCLUSION

In this experiment, the interference and diffraction of light were measured for the multiple and single photon cases. The measured intensity profile matched well with the theoretical intensity profile. At first, the simple fitting based on the theory of wave optics was conducted, assuming the monochromatic light. The fitting was suitable enough to confirm that the experimental data is in form of the fitting equation. For the slit No. 14, the two slits are tested whether their widths are identical or not. Since the 95 % confidence interval didn't include each other for the multiple photon case, the widths seems to be slightly different. To improve the fitting accuracy, the bandwidth effect was considered and it predicted the nonzero intensity of minima well for the multiple photon case. On the contrary, for the single photon case, the decoherence effect is predominant over the bandwidth effect. To fit the intensity profile of the asymmetric double slit, the Fresnel diffraction model was developed. This model predicts the overall experimental result well, however, its computational cost is too large and reaching the convergence is challenging. The most important conclusion is that the wave-particle duality of light was confirmed. The wave-like property exists not only in the macroscopic light but also a single photon. Namely, the wave-like property is an intrinsic feature of a photon.

ACKNOWLEDGMENTS

I appreciate performing this harsh experiment with my dear coworkers, Seunghyun Moon and Gyujin Kim.

[1] T. L. Dimitrova and A. Weis, The wave-particle duality of light: A demonstration experiment, American Journal of Physics **76**, 137 (2008).
[2] E. Hecht, *Optics* (Pearson Education India, 2012).
[3] R. Foord, R. Jones, C. Oliver, and E. Pike, The use of photomultiplier tubes for photon counting, Applied optics **8**, 1975 (1969).